Int. J. Electrochem. Sci., 10 **(2015)** 3010 - 3025

International Journal of ELECTROCHEMICAL SCIENCE
www.electrochemsci.org

New pyrimidothiazine Derivative as Corrosion Inhibitor for Carbon Steel in Acidic Media

M. Belayachi[1], *H. Serrar*[2], *H. Zarrok*[1], *A. El Assyry*[5], *A. Zarrouk*[3,*], *H. Oudda*[1], *S. Boukhris*[2], *B. Hammouti*[3,4], *Eno E. Ebenso*[6,*], *A. Geunbour*[7]

[1] Laboratoire des procèdes de séparation, Faculté des Sciences, Université Ibn Tofail, Kenitra, BP 133, Kenitra, Morocco.
[2] Laboratoire de Synthèse Organique, Organométallique et Théorique. Université Ibn Tofail. Faculté des Sciences. BP 133, Kenitra. Morocco.
[3] LCAE-URAC18, Faculté des Sciences, Université Mohammed 1er, Oujda, Morocco.
[4] Petrochemical Research Chair, Chemistry Department, College of Science, King Saud University, P.O. Box 2455, Riyadh 11451, Saudi Arabia.
[5] Laboratoire d'Optoélectronique et de Physico-chimie des Matériaux (Unité associée au CNRST), Département de Physique,Université Ibn Tofail, B.P. 133, Kénitra, Maroc.
[6] Material Science Innovation & Modelling (MaSIM) Research Focus Area, Faculty of Agriculture, Science and Technology, North-West University (Mafikeng Campus), Private Bag X2046, Mmabatho 2735, South Africa
[7] Laboratoire Corrosion- Électrochimie, Faculté des Sciences, Université Mohamed V, BP. 1014 Rabat, Maroc.
*E-mail: azarrouk@gmail.com, Eno.Ebenso@nwu.ac.za

Received: 28 November 2014 / *Accepted:* 5 February 2015 / *Published:* 24 February 2015

2,8-bis(4-chlorophenyl)-3-hydroxy-4,6-dioxo-4,6-dihydropyrimido[2,1-b][1,3]thiazine-7-carbonitrile (CHPTC) was tested as corrosion inhibitor for carbon steel in 2.0 M H_3PO_4 by using polarization, electrochemical impedance spectroscopy (EIS) and computational calculations. Potentiodynamic polarization curves indicated that the pyrimidothiazine derivativeas mixed-type inhibitor. Impedance measurements showed that the double-layer capacitance decreased and charge-transfer resistance increased with increase in the inhibitor concentration and hence increasing in inhibition efficiency. The effect of temperature on the corrosion behavior of carbon steel in 2.0 M H_3PO_4 with and without addition of CHPTC was studied in the temperature range 313-333 K. The adsorption of the inhibitor molecules was in accordance with the Langmuir adsorption isotherm. Quantum chemical approach used to calculate electronic properties of the molecule to ascertain the relation between inhibitive effect and molecular structure.

Keywords: Pyrimidothiazine derivative, Steel, Corrosion inhibition, Electrochemical techniques, DFT.

1. INTRODUCTION

Acid solutions are generally used for the removal of undesirable scale and rust in several industrial processes. Hydrochloric and sulphuric acids are widely used in the pickling processes of metals. Several methods are present for corrosion prevention. Use of inhibitors is one of the most practical methods for protection against corrosion especially in acid solutions to prevent metal dissolution and acid consumption [1]. Most effective inhibitors are organic compounds containing electronegative functional groups and π electrons in triple or conjugated double bonds [2-23]. These compounds also have heteroatoms (such as N, P, O, and S) and aromatic rings in their structure, which are the major adsorption centers [24-26]. In view of this, several inhibitors have been synthesized and used successfully to inhibit corrosion of metals in acid media.

Theoretical calculations have been used recently to explain the mechanism of corrosion inhibition, which proved to be a very powerful tool in this direction [27-30]. The geometry of inhibitor molecule in its ground state, the nature of its molecular orbitals HOMO (Highest Occupied Molecular Orbital) and LUMO (Lowest Unoccupied Molecular Orbital) are directly involved in the corrosion inhibition activity.

In continuation of our previous study, the present work devotes to investigate the adsorption and corrosion inhibition of 2,8-bis(4-chlorophenyl)-3-hydroxy-4,6-dioxo-4,6-dihydropyrimido[2,1-b][1,3]thiazine-7-carbonitrile (CHPTC) on carbon steel in phosphoric acid by potentiodynamic polarization, electrochemical impedance spectroscopy (EIS) and quantum chemical calculations in detail. The molecular structure of this pyrimidothiazine derivative is shown in Fig 1.

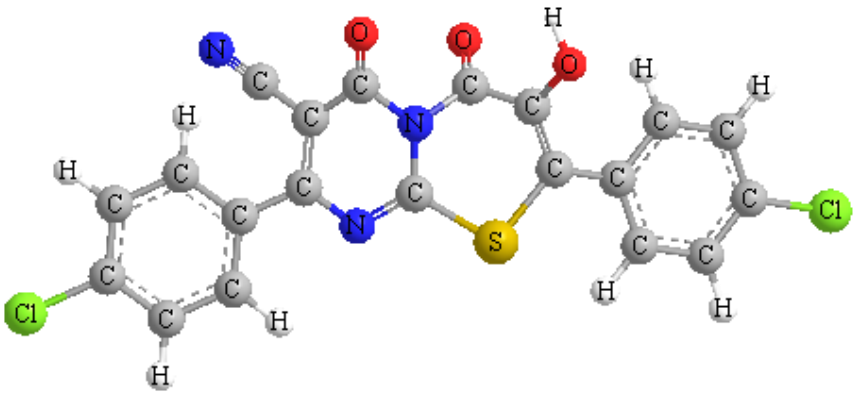

Figure 1. The chemical structure of the studied pyrimidothiazine derivative.

2. EXPERIMENTAL METHODS

2.1. Materials

The steel used in this study is a carbon steel (CS) (Euronorm: C35E carbon steel and US specification: SAE 1035) with a chemical composition (in wt%) of 0.370 % C, 0.230 % Si, 0.680 % Mn, 0.016 % S, 0.077 % Cr, 0.011 % Ti, 0.059 % Ni, 0.009 % Co, 0.160 % Cu and the remainder iron (Fe).

2.2. Solutions

The aggressive solutions of 2.0 M H_3PO_4 was prepared by dilution of analytical grade 85% H_3PO_4 with distilled water. The organic compound tested is 2,8-bis(4-chlorophenyl)-3-hydroxy-4,6-dioxo-4,6-dihydropyrimido[2,1-b][1,3]thiazine-7-carbonitrile (CHPTC). The concentration range of this compound was 10^{-3} to 10^{-6} M.

2.3. Polarization measurements

2.3.1. Electrochemical impedance spectroscopy

The electrochemical measurements were carried out using Volta lab (Tacussel- Radiometer PGZ 100) potentiostate and controlled by Tacussel corrosion analysis software model (Voltamaster 4) at under static condition. The corrosion cell used had three electrodes. The reference electrode was a saturated calomel electrode (SCE). A platinum electrode was used as auxiliary electrode of surface area of 1 cm^2. The working electrode was carbon steel. All potentials given in this study were referred to this reference electrode. The working electrode was immersed in test solution for 30 minutes to a establish steady state open circuit potential (*E*ocp). After measuring the *E*ocp, the electrochemical measurements were performed. All electrochemical tests have been performed in aerated solutions at 303 K. The EIS experiments were conducted in the frequency range with high limit of 100 kHz and different low limit 0.1 Hz at open circuit potential, with 10 points per decade, at the rest potential, after 30 min of acid immersion, by applying 10 mV ac voltage peak-to-peak. Nyquist plots were made from these experiments. The best semicircle can be fit through the data points in the Nyquist plot using a non-linear least square fit so as to give the intersections with the *x*-axis.

The inhibition efficiency of the inhibitor was calculated from the charge transfer resistance values using the following equation:

$$\eta_z\% = \frac{R_{ct}^{i} - R_{ct}^{\circ}}{R_{ct}^{i}} \times 100 \quad (1)$$

where R_{ct}° and R_{ct}^{i} are the charge transfer resistance in absence and in presence of inhibitor, respectively.

2.3.2. Potentiodynamic polarization

The electrochemical behaviour of carbon steel sample in inhibited and uninhibited solution was studied by recording anodic and cathodic potentiodynamic polarization curves. Measurements were performed in the 2.0 M H_3PO_4 solution containing different concentrations of the tested inhibitor by changing the electrode potential automatically from -900 to -100 mV versus corrosion potential at a scan rate of 2 mV s^{-1}. The linear Tafel segments of anodic and cathodic curves were extrapolated to corrosion potential to obtain corrosion current densities (I_{corr}). From the polarization curves obtained, the corrosion current (I_{corr}) was calculated by curve fitting using the equation:

$$I = I_{corr}\left[exp\left(\frac{2.3\Delta E}{\beta_a}\right) - exp\left(\frac{2.3\Delta E}{\beta_c}\right)\right] \quad (2)$$

The inhibition efficiency was evaluated from the measured I_{corr} values using the relationship:

$$\eta_{IE}\% = \frac{I_{corr} - I_{corr(i)}}{I_{corr}} \times 100 \quad (3)$$

where, I_{corr} and $I_{corr(i)}$ are the corrosion current density in absence and presence of inhibitor, respectively.

2.4. Quantum chemical calculations

Complete geometrical optimizations of the investigated molecules are performed using DFT (density functional theory) with the Beck's three parameter exchange functional along with the Lee-Yang-Parr nonlocal correlation functional (B3LYP) [31-33] with 6-31G* basis set is implemented in Gaussian 03 program package [34]. This approach is shown to yield favorable geometries for a wide variety of systems. This basis set gives good geometry optimizations. The geometry structure was optimized under no constraint. The following quantum chemical parameters were calculated from the obtained optimized structure: The highest occupied molecular orbital (E_{HOMO}) and the lowest unoccupied molecular orbital (E_{LUMO}), the energy difference (ΔE) between E_{HOMO} and E_{LUMO}, dipole moment (μ), electron affinity (A), ionization potential (I) and the fraction of electrons transferred (ΔN).

3. RESULTS AND DISCUSSION

3.1. Electrochemical impedance spectroscopy measurements

The corrosion behavior of carbon steel in 2.0 M H_3PO_4, in absence and the presence of various concentrations of CHPTC were also investigated by EIS technique. The resultant Nyquist plots are shown in Fig. 2. The values of inhibition efficiency (η_Z%) were calculated by the equation 1. To obtain the values of double layer capacitance (C_{dl}), the values of frequency at which the imaginary component of the impedance is maximum $-Z_{im(max)}$ was found and used in the following equation with corresponding R_{ct} values:

$$C_{dl} = \frac{1}{2\pi f_{max} R_{ct}} \quad (4)$$

Nyquist plots contain semicircle with centre under real axis. The size of the semicircle increases with the inhibitor concentration, indicating the charge transfer process as the main controlling factor for the corrosion inhibition of carbon steel. It is apparent from the plots that, the impedance of the inhibited solution has increased with the increase in the concentration of the inhibitor.

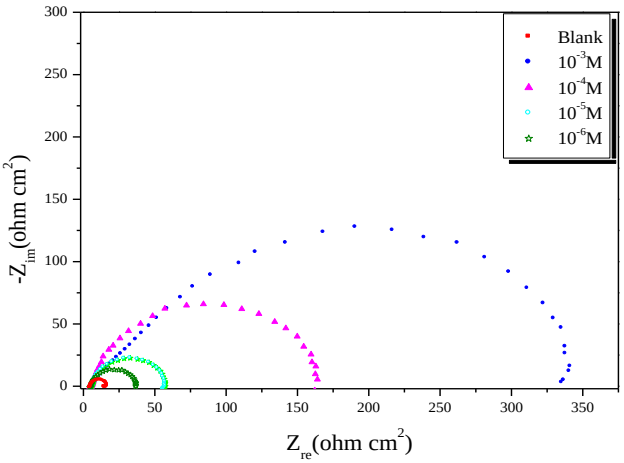

Figure 2. Nyquist plots for carbon steel in 2.0 M phosphoric acid solution at 303 K containing various concentrations of the inhibitor.

The experimental results of EIS measurements for the corrosion of carbon steel in 2.0 M phosphoric acid in the absence and presence of inhibitor are given in Table 1. As it can be observed from the table, the charge transfer resistance (R_{ct}) value increased with increase in the concentration of the inhibitor. Whereas values of the capacitance of the interface (C_{dl}) starts decreasing, with increase in inhibitor concentration, which is most probably due to the decrease in local dielectric constant and/or increase in thickness of the electrical double layer. This suggests that the inhibitor acts via adsorption at the metal/solution interface [35] and the decrease in the C_{dl} values is caused by the gradual replacement of water molecules by the adsorption of the inhibitor molecules on the electrode surface, which decreases the extent of metal dissolution [36].

Table 1. AC impedance data of carbon steel in 2.0 M phosphoric acid solution at 303 K.

Conc (M)	R_{ct} (Ω cm^2)	C_{dl} (μF/cm^2)	η_z (%)
2.0	11.8	118.8	-----
10^{-3}	366.1	14.5	96.8
10^{-4}	161.7	50.0	92.7
10^{-5}	53.0	96.1	77.7
10^{-6}	32.6	99.0	63.8

3.2. Potentiodynamic polarization measurements

3.2.1. Effect of concentration inhibitor

Fig. 3 shows anodic and cathodic polarization plot of carbon steel in 2.0 M H_3PO_4 in the absence and in the presence of CHPTC inhibitor of different concentrations at 303 K. Table 2 shows

the electrochemical corrosion parameters such as corrosion potential (E versus SCE), corrosion current density (I_{corr}) and the inhibition efficiency (η_{IE}%).

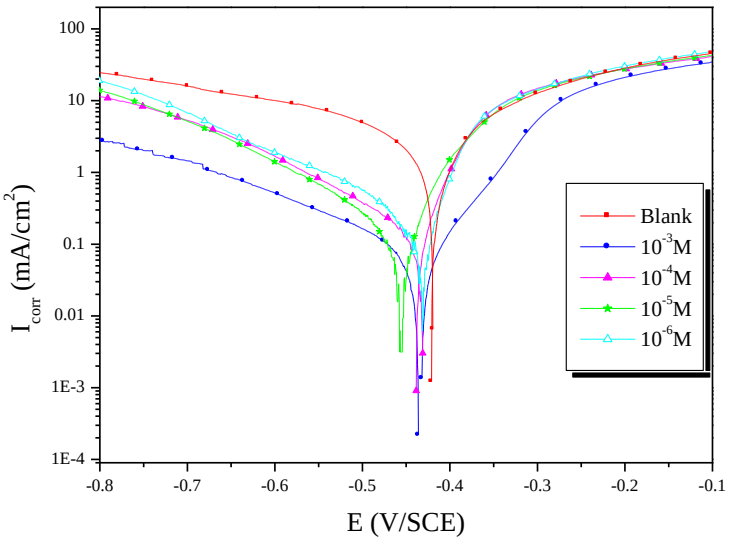

Figure 3. Tafel polarization curves for the corrosion of carbon steel in 2.0 M phosphoric acid containing different concentrations of CHPTC at 303 K.

Table 2. Potentiodynamic polarization parameters for the corrosion of carbon steel in 2.0 M phosphoric acid without and with different concentrations of CHPTC at 303 K.

Conc (M)	-E (mv/SCE)	$-\beta_c$ (mv/dec)	I_{corr} ($\mu A/cm^2$)	η_{IE} (%)
Blank	418.6	224.0	2169.1	-----
10^{-3}M	425.2	198.8	53.3	97.5
10^{-4}M	452.4	175.3	161.1	92.6
10^{-5}M	456.5	171.5	187.4	91.1
10^{-6}M	432.2	207.0	290.5	86.6

Figure 3 illustrates the polarization curves of carbon steel in 2.0 M H_3PO_4 solution without and with various concentrations of CHPTC at 303K. The presence of CHPTC shifts both anodic and cathodic branches to the lower values of corrosion current densities and thus causes a remarkable decrease in the corrosion rate. In 2.0 M H_3PO_4 solution, the presence of CHPTC causes a remarkable decrease in the corrosion rate i.e., shifts both anodic and cathodic curves to lower current densities. In other words, both cathodic and anodic reactions of carbon steel electrode are retarded by CHPTC in phosphoric acid solution. However, for potential higher than -250 mVSCE, the presence of CHPTC did not change the current-vs.-potential characteristics in anodic domain (Fig. 3). This potential can be defined as the desorption potential. The phenomenon may be explained by the equality of the rate of adsorption of inhibitor and that of the metal oxidation leading to a desorption of the inhibitor molecule

from the electrode surface [37]. The Tafel slopes of β_c at 303 K change remarkably upon addition of ACPTC which indicates that the presence of CHPTC change the mechanism of hydrogen evolution and the metal dissolution process. Generally, an inhibitor can be classified as cathodic or anodic type if the shift of corrosion potential in the presence of the inhibitor is more than 85 mV with respect to that in the absence of the inhibitor [38, 39]. In the presence of CHPTC, E shifts to less negative (about 38 mV) which indicates that CHPTC can be arranged as mixed type inhibitor, with predominant cathodic effectiveness.

3.3.2. Effect of temperature

The influence of temperature is also studied by potentiodynamic polarization. The polarization curves for carbon steel electrode in 2.0 M H_3PO_4 in the absence and in the presence of 1.0 mM of CHPTC in the temperature range 313-333 K are given in Figs. 4 and 5, respectively.

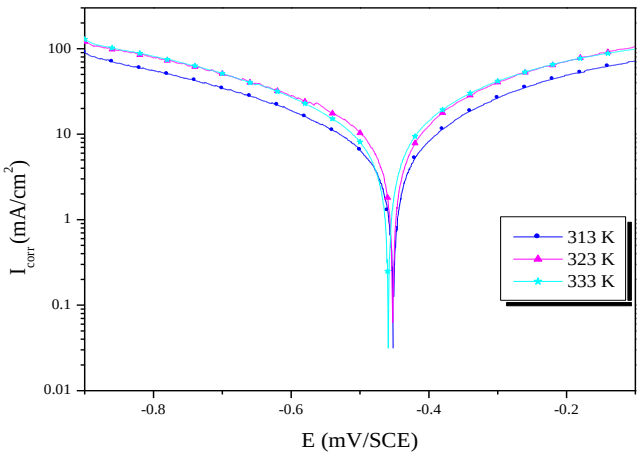

Figure 4. Polarization curves for carbon steel in 2.0 M H_3PO_4 at different temperatures.

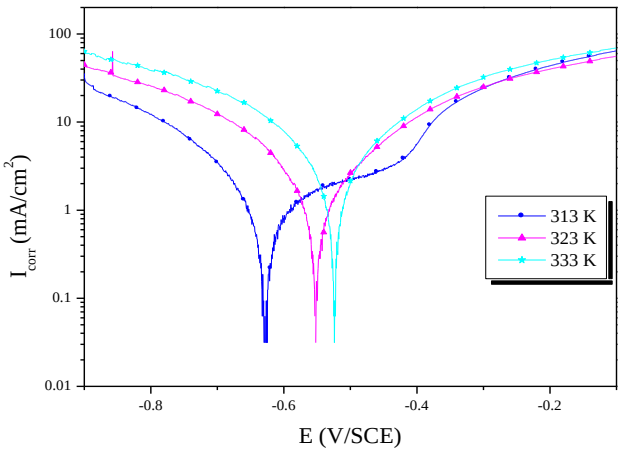

Figure 5. Polarization curves for carbon steel in 2.0 M H_3PO_4 containing 1.0 mM of CHPTC at different temperatures.

The results deduced from the polarization curves are given in Table 3. As it can be seen, that raising the temperature increases both anodic and cathodic reactions of carbon steel electrode both in the absence and in the presence of extract. It is seen from Table 3 that the corrosion current density (I_{corr}) increased with the increasing temperature; although the pyrimidothiazine derivative investigated have been inhibiting properties at all temperatures studied. The inhibition efficiency of CHPTC reaches a maximum value (82.8%) at 313 K, upon increasing the temperature, η_{IE} % is slightly decreased and the pyrimidothiazine derivative becomes less effective at 333 K. This behavior shows again the physical nature of adsorption of CHPTC in H_3PO_4 solution.

Table 3. Polarization parameters and the corresponding inhibition efficiency for carbon steel in 2.0 M H_3PO_4 in the absence and presence of 1.0 mM CHPTC at different temperatures.

Temp (K)	E (mV/SCE)	$-\beta_c$ (mV/dec)	I_{corr} ($\mu A/cm^2$)	η_{IE} (%)
313	452.5	332	4910.5	-----
323	453.3	129	6826.8	-----
333	459.8	305	9390.0	-----
313	628.8	174	1175.1	82.8
323	553.1	194	2292.0	80.2
333	524.9	184	3167.7	66.3

The activation energies, E_a, were calculated from an Arrhenius-type plot (Eq. (5)) [40,41]:

$$I_{corr} = k \exp\left(-\frac{E_a}{RT}\right) \quad (5)$$

where E_a is the apparent activation corrosion energy, T is the absolute temperature, k is the Arrhenius pre-exponential constant and R is the universal gas constant.

The enthalpy of activation, ΔH_a, and the entropy of activation, ΔS_a, were calculated from equation (6):

$$I_{corr} = \frac{RT}{Nh} \exp\left(\frac{\Delta S_a}{R}\right) \exp\left(\frac{\Delta H_a}{RT}\right) \quad (6)$$

where h is Planck's constant, N is Avogadro's number, ΔS_a is the entropy of activation and ΔH_a is the enthalpy of activation.

Plots of Ln (I_{corr}) vs. 1000/T and Ln (I_{corr}/T) vs. 1000/T gave straight lines with slopes of $-E_a/R$ and $-\Delta H_a/R$, respectively. The intercepts were A and [Ln (R/Nh) + (ΔS_a/R)] for the Arrhenius and transition state equations, respectively. Figs. 6 and 7 represent the data plots of Ln (I_{corr}) vs. 1000/T and Ln (I_{corr}/T) vs. 1000/T in the absence and presence of 1.0 mM CHPTC, representative example. The calculated values from both methods of the activation energy, E_a, the enthalpy of activation, ΔH_a, and the entropy of activation, ΔS_a, are tabulated in Table 4.

Inspection of Table 4 shows that values of both E_a, ΔH_a obtained in presence of CHPTC are higher than those obtained in the inhibitor-free solution. This observation further supports the proposed physical adsorption mechanism.

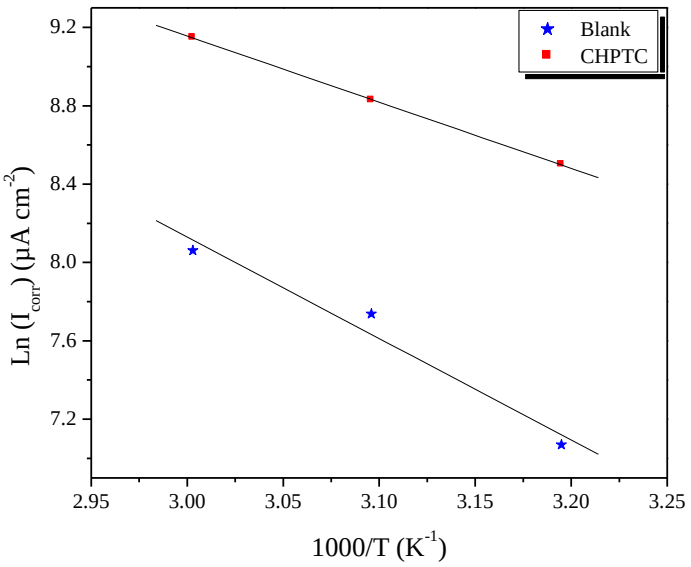

Figure 6. Arrhenius plots of carbon steel in 2.0 M H_3PO_4 with and without 1.0 mM of CHPTC.

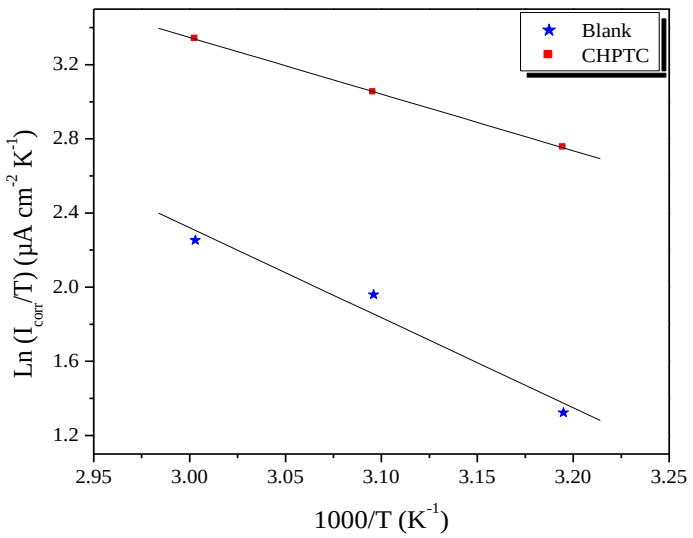

Figure 7. Relation between Ln (I_{corr}/ T) and 1000/T at different temperatures.

Table 4. Activation parameters, E_a, ΔH_a and ΔS_a, of the dissolution of carbon steel in 2.0 M H_3PO_4 in the absence and the presence of 1.0 mM of CHPTC.

Inhibitor	E_a (kJ/mol)	ΔH_a (kJ/mol)	ΔS_a (J mol^{-1} K^{-1})
Blank	28.08	25.40	-93.51
CHPTC	43.11	40.42	-56.97

Higher values of E_a in inhibited systems compared to the blank have been reported [42,43] to be indicative of physical adsorption mechanism, while lower values of E_a suggest a chemisorption mechanism. On the other hand, the positive sign of ΔH_a reflects the endothermic nature of the carbon steel dissolution process suggesting that the dissolution of carbon steel is slow [44] in the presence of inhibitor. This behaviour can be explained as a result of the replacement process of water molecules during adsorption of CHPTC on steel surface [45,46].

The large negative value of ΔS_a for carbon steel in 2.0 M H_3PO_4 implies that the activated complex is the rate-determining step, rather than the dissociation step. In the presence of the inhibitor, the value of ΔS_a increases and is generally interpreted as an increase in disorder as the reactants are converted to the activated complexes [47].

3.3.3. Adsorption isotherm

The adsorption isotherm that describes the adsorptive behavior of organic inhibitors is important in order to know the mechanism of corrosion inhibition. Basic information dealing with interaction between the inhibitor molecules and the metal surface can be provided by adsorption isotherms. Several adsorption isotherms were attempted to fit the degree of surface coverage values (θ) to adsorption isotherms including Frumkin, Temkin, Freundlich and Langmuir isotherms. The θ values for various concentrations of inhibitors in acidic media have been evaluated from the polarization measurements. The best fit was obtained in the case of Langmuir isotherm which assumes that the solid surface contains a fixed number of adsorption sites and each site holds one adsorbed species [48]. The plot of C_{inh}/θ vs. C_{inh} (Fig. 8) yields a straight line with correlation coefficient of 0.99999 providing that the adsorption of CHPTC from 2.0 M H_3PO_4 solution on the carbon steel surface obeys Langmiur adsorption isotherm. This isotherm can be represented as:

$$\frac{C_{\text{inh}}}{\theta} = \frac{1}{K_{\text{ads}}} + C_{\text{inh}} \qquad (7)$$

where C_{inh} is the molar concentration of the inhibitor and K_{ads} is the equilibrium constant for the adsorption-desorption process. The value of K_{ads} was found to be 489787.92 M^{-1}. The relatively high value of adsorption equilibrium constant reflects the high adsorption ability of CHPTC on carbon steel surface [49]. The K_{ads} is related to the standard free energy of adsorption, ΔG°_{ads}, by the following equation:

$$K_{ads} = (\frac{1}{55.5}) \exp(-\frac{\Delta G^{\circ}_{ads}}{RT}) \qquad (8)$$

where R is gas constant and T is absolute temperature of experiment and the constant value of 55.5 is the concentration of water in solution in mol L^{-1}.

The ΔG°_{ads} was calculated as -43.12 kJ mol^{-1}. The negative value of ΔG°_{ads} indicates the spontaneity of the adsorption process and the stability of adsorbed layer on the carbon steel

surface. It is well known that the values of ΔG°_{ads} of the order of -20 kJ mol^{-1} or lower indicate a physisorption; those of order of -40 kJ mol^{-1} or higher involve charge sharing or transfer from the inhibitor molecules to the metal surface to form a coordinate type of bond (chemisorption) [50-52]. On the other hand, the adsorption phenomenon of an organic molecule is not considered only as a purely physical or chemical adsorption phenomenon [53,54]. A wide spectrum of conditions, ranging from the dominance of chemisorption or electrostatic effects, arises from other adsorptions experimental data [55]. The value of -43.12 kJ mol^{-1} may suggest chemisorption mode.

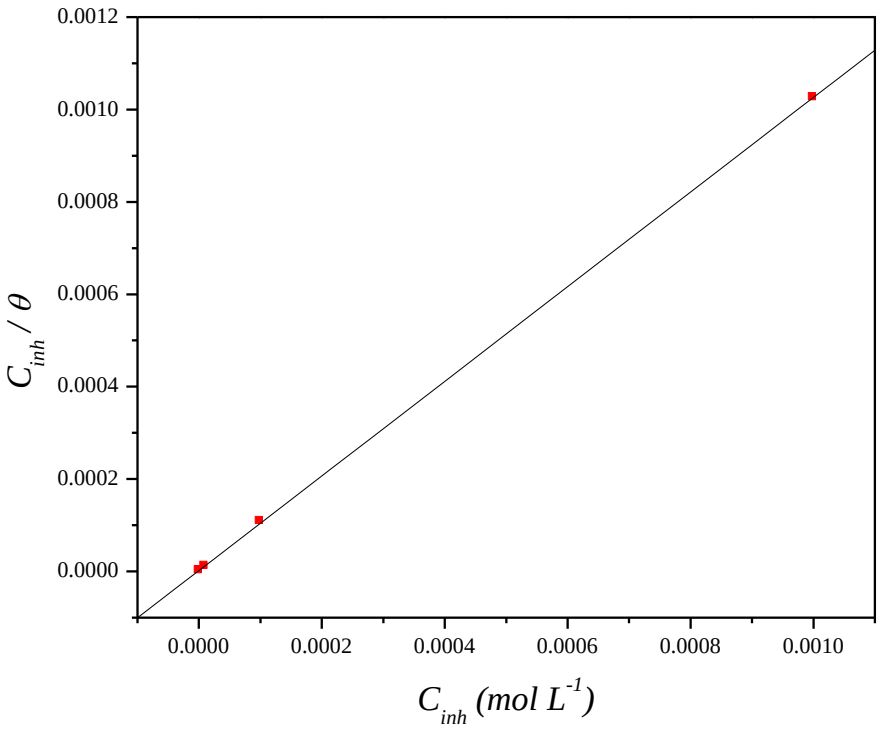

Figure 8. Langmuir adsorption of CHPTC on the carbon steel surface in 2.0 M H_3PO_4 solution.

3.3. Quantum Chemical Calculations

Quantum chemical calculations are utilized to ascertain whether there is a clear relationship between the molecular structure of the synthesized inhibitor and its inhibition effect. The structure parameters of the synthesized inhibitor are used to elucidate the inhibition mechanism in the present work. The equilibrium geometry structures and the frontier molecule orbital density distributions of the molecule are shown in Fig. 9 and the quantum chemical parameters are listed in Table 5.

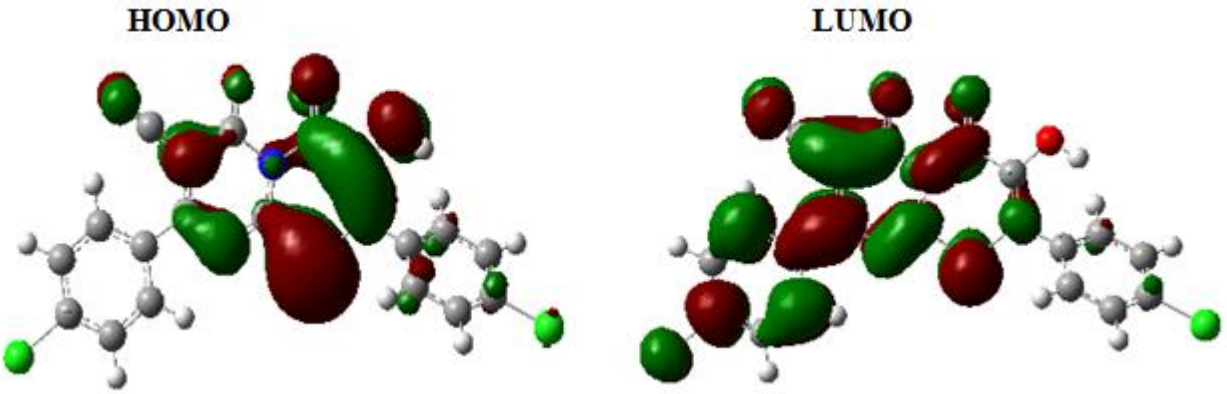

Figure 9. Frontier molecule orbital density distributions of the synthesized inhibitor.

E_{HOMO} is often associated with the capacity of a molecule to donate electron. High value of E_{HOMO} probably indicates a tendency of the molecule to donate electrons to appropriate acceptor molecules with low energy and empty molecular orbital. E_{LUMO} indicates the ability of the molecule to accept electrons. The lower the value of E_{LUMO}, the more probable is that the molecule would accept electrons [56]. According to frontier orbital theory, the reaction of reactants mainly occurs on HOMO and LUMO [57]. So, the smaller gap (ΔE) between E_{HOMO} and E_{LUMO} is the more probable to donate and accept electrons. The values of ΔE in Table 5, suggesting the strongest ability of the synthesized inhibitor to form coordinate bonds with d-orbital of metal through donating and accepting electrons, is in good agreement with the experimental results. Additionally, for the dipole moment (μ), higher value of μ will favor the enhancement of corrosion inhibition [58]. From Table 5, the value of μ is higher, which is also in agreement with the experimental results mentioned above.

Another method to correlate inhibition efficiency with parameters of molecular structure is to calculate the fraction of electrons transferred from inhibitor to metal surface. According to Koopman's theorem [59], E_{HOMO} and E_{LUMO} of the inhibitor molecule are related to the ionization potential (I) and the electron affinity (A), respectively. The ionization potential (I) and the electron affinity (A) are defined as follows:

$$I = -E_{HOMO} \quad (9)$$

$$A = -E_{LUMO} \quad (10)$$

Then absolute electronegativity (χ) and global hardness (η) of the inhibitor molecule are approximated as follows [60]:

$$\chi = \frac{I + A}{2} \quad (10)$$

$$\eta = \frac{I - A}{2} \quad (11)$$

Thus the fraction of electrons transferred from the inhibitor to metallic surface, ΔN, is given by [61]:

$$\Delta N = \frac{\chi_{Fe} - \chi_{inh}}{2(\eta_{Fe} + \eta_{inh})} \quad (12)$$

To calculate the fraction of electrons transferred the theoretical values of of χ_{Fe} (7 eV mol^{-1}) and of η_{Fe} (0 eV mol^{-1}) are used [62]. The calculated results are presented in Table 5.

Table 5. Calculated quantum chemical parameters of the studied compound.

Quantum parameters	CHPTC
E_{HOMO} (eV)	-7.7008
E_{LUMO} (eV)	-5.7688
ΔE gap (eV)	1.9320
μ (debye)	12.5061
$I = -E_{HOMO}$	7.7008
$A = -E_{LUMO}$	5.7688
$\chi = \frac{I + A}{2}$	6.7348
$\eta = \frac{I - A}{2}$	0.9660
$\Delta N = \frac{\chi_{Fe} - \chi_{inh}}{2(\eta_{Fe} + \eta_{inh})}$	0.5000
TE (eV)	-67018.0176

Generally, value of ΔN shows inhibition efficiency resulting from electron donation, and the inhibition efficiency increases with the increase in electron-donating ability to the metal surface. Value of ΔN show inhibition effect resulted from electrons donation. According to Lukovits's study [63], if $\Delta N < 3.6$, the inhibition efficiency increases with increasing electron-donating ability at the metal surface.

Based on these calculations, it is expected that the synthesized inhibitor is donor of electrons, and the steel surface is the acceptor, and this favors chemical adsorption of the inhibitor on the electrode surface. Here the inhibitor binds to the steel surface and forms an adsorption layer against corrosion. The synthesized inhibitor shows the highest inhibition efficiency because it has the highest HOMO energy and this reflects the greatest ability (the lowest ΔE) of offering electrons. It can be seen from Table 5 that the ability of the synthesized inhibitor to donate electrons to the metal surface, which is in good agreement with the higher inhibition efficiency of the synthesized inhibitor.

4. CONCLUSION

2,8-bis(4-chlorophenyl)-3-hydroxy-4,6-dioxo-4,6-dihydropyrimido[2,1-b][1,3]thiazine-7-carbonitrile (CHPTC) was found to be an inhibitor for the corrosion of carbon steel in HCl solution.

Inhibition efficiency increases with increase in CHPTC concentration, but decrease with increase in temperature.

Double-layer capacitances decrease with respect to blank solution when the synthesized inhibitor is added. This fact can be explained by adsorption of the synthesized inhibitor species on the steel surface. Polarization studies reveal that CHPTC act as a mixed-type inhibitor with predominant cathodic effectiveness. The adsorption CHPTC on carbon steel surface can be approximated by Langmuir isotherm model. The smaller gap between E_{HOMO} and E_{LUMO} favors the adsorption of the synthesized inhibitor on iron surface and enhancement of corrosion inhibition.

ACKNOWLEDGEMENTS
Prof S. S. Al-Deyab and Prof B. Hammouti extend their appreciation to the Deanship of Scientific Research at king Saud University for funding the work through the research group project.

References

1. J.M. Sykes, *Brit. Corros. J*. 25 (1990) 175.
2. A. Zarrouk, B. Hammouti, H. Zarrok, R. Salghi, A. Dafali, Lh. Bazzi, L. Bammou, S. S. Al-Deyab, *Der Pharm. Chem*. 4 (2012) 337.
3. H. Zarrok, R. Saddik, H. Oudda, B. Hammouti, A. El Midaoui, A. Zarrouk, N. Benchat, M. Ebn Touhami, *Der Pharm. Chem*. 3 (2011**)** 272.
4. A. Zarrouk, B. Hammouti, A. Dafali, H. Zarrok, *Der Pharm. Chem*. 3 (2011) 266.
5. A. Ghazoui, R. Saddik, N. Benchat, B. Hammouti, M. Guenbour, A. Zarrouk, M. Ramdani, *Der Pharm. Chem*. 4 (2012) 352.
6. A. Zarrouk**,** B. Hammouti, H. Zarrok, I. Warad, M. Bouachrine, *Der Pharm. Chem*. 3 (2011) 263.
7. D. Ben Hmamou, R. Salghi, A. Zarrouk, M. Messali, H. Zarrok, M. Errami, B. Hammouti, Lh. Bazzi , A. Chakir, *Der Pharm. Chem*. 4 (2012) 1496.
8. H. Bendaha, A. Zarrouk, A. Aouniti, B. Hammouti, S. El Kadiri, R. Salghi, R. Touzani, *Phys. Chem. N*ews, 64 (2012) 95.
9. S. Rekkab, H. Zarrok, R. Salghi, A. Zarrouk**,** Lh. Bazzi, B. Hammouti, Z. Kabouche, R. Touzani, M. Zougagh, *J. Mater. Environ. Sci*. 3 (2012) 613.
10. H. Zarrok, A. Zarrouk, R. Salghi, Y. Ramli, B. Hammouti, M. Assouag, E. M. Essassi, H. Oudda and M. Taleb, *J. Chem. Pharm. Res*. 4 (2012) 5048.
11. A. Zarrouk, B. Hammouti, T. Lakhlifi, M. Traisnel, H. Vezin, F. Bentiss, *Corros. Sci*. 90 (2015) 572.
12. Y. ELaoufir, H. Bourazmi, H. Serrar, H. Zarrok, A. Zarrouk, B. Hammouti, A. Guenbour, S. Boukhriss, H. Oudda, *Der Pharma. Lett.* 6 (2014) 526.
13. A. Zarrouk, B. Hammouti, H. Zarrok, S.S. Al-Deyab, S.S., I. Warad, *Res. Chem. Intermed*. 38 (2012) 1655.
14. H. Zarrok, A. Zarrouk, R. Salghi, B. Hammouti, M. Elbakri, M. Ebn touhami, F. Bentiss, H. Oudda, *Res. Chem. Intermed*. 40 (2014) 801.
15. A. Zarrouk, B. Hammouti, A. Dafali, F. Bentiss, *Ind. Eng. Chem. Res.* (2013) 2560.
16. H. Zarrok, A. Zarrouk, R. Salghi, H. Oudda, B. Hammouti, M. EbnTouhami, M. Bouachrine, O.H. Pucci, *Port. Electrochim. Acta*, 30 (2012) 405.
17. D. Ben Hmamou, M. R. Aouad, R. Salghi, A. Zarrouk, M. Assouag, O. Benali, M. Messali, H. Zarrok, B. Hammouti, *J. Chem. Pharm. Res*. 4 (2012) 3489.
18. L. Afrine, A. Zarrouk, H. Zarrok, R. Salghi, R. Touir, B. Hammouti, H. Oudda, M. Assouag, H. Hannache, M. El Harti, M. Bouachrine, *J. Chem. Pharm. Res*. 5 (2013) 1474.

19. A. Zarrouk, H. Zarrok, R. Salghi, R. Touir, B. Hammouti, N. Benchat, L. Afrine, H. Hannache, M. El Hezzat, M. Bouachrine, *J. Chem. Pharm. Res*. 5 (2013) 1482.
20. H. Zarrok, H. Oudda, A. El Midaoui, A. Zarrouk, B. Hammouti, M. Ebn Touhami, A. Attayibat, S. Radi, R. Touzani, *Res. Chem. Intermed*. 38 (2012) 2051.
21. A. Ghazoui, A. Zarrouk, N. Bencaht, R. Salghi, M. Assouag, M. El Hezzat, A. Guenbour, B. Hammouti, *J. Chem. Pharm. Res*. 6 (2014) 704.
22. D. Ben Hmamou, R. Salghi, A. Zarrouk, B. Hammouti, S.S. Al-Deyab, Lh. Bazzi, H. Zarrok, A. Chakir, L. Bammou, *Int. J. Electrochem. Sci*. 7 (2012) 2361.
23. H. Zarrok, A. Zarrouk, B. Hammouti, R. Salghi, C. Jama, F. Bentiss, *Corros. Sci*. 64 (2012) 243
24. Z.H. Tao, S.T. Zhang, W.H. Li, B.R. Hou, *Corros. Sci*. 51 (2009) 2588.
25. M. Lebrini, F. Robert, H. Vezin, C. Roos, *Corros. Sci*. 52 (2010) 3367.
26. M. Abdallah, *Corros. Sci*. 46 (2004) 1981.
27. J.P. Chopart, J. Douglade, P. Fricoteaux, A. Olivier, *Electrochim. Acta*, 36 (1991) 459.
28. M.D. Pritzker, T.Z. Fahidy, Electrochim. Acta 37 (1992) 103.
29. S. Magiano, *Electrochim. Acta*, 42 (1997) 377.
30. S. Krzewska, *Electrochim. Acta*, 42 (1997) 3531
31. A. D. Becke, *J. Chem. Phy*. 96 (1992) 9489.
32. A. D. Becke, *J. Chem. Phy*. 98 (1993) 1372.
33. C. Lee, W. Yang, R.G. Parr, *Phy. Rev. B* 37 (1988) 785.
34. M.J. Frisch, G.W. Trucks, H.B. Schlegel, G.E. Scuseria, M.A. Robb, J.R. Cheeseman, J.A. Montgomery Jr., T. Vreven, K.N. Kudin, J.C. Burant, J.M. Millam, S.S. Iyengar, J. Tomasi, V. Barone, B. Mennucci, M. Cossi, G. Scalmani, N. Rega, G.A. Petersson, H. Nakatsuji, M. Hada, M. Ehara, K. Toyota, R. Fukuda, J. Hasegawa, M. Ishida, T. Nakajima, Y. Honda, O. Kitao, H. Nakai, M. Klene, X. Li, J.E. Knox, H.P. Hratchian, J.B. Cross, C. Adamo, J. Jaramillo, R. Gomperts, R.E. Stratmann, O. Yazyev, A.J. Austin, R. Cammi, C. 870 H. Ju et al. / Corrosion Science 50 (2008) 865-871 Pomelli, J.W. Ochterski, P.Y. Ayala, K. Morokuma, G.A. Voth, P. Salvador, J.J. Dannenberg, V.G. Zakrzewski, S. Dapprich, A.D. Daniels, M.C. Strain, O. Farkas, D.K. Malick, A.D. Rabuck, K. Raghavachari, J.B. Foresman, J.V. Ortiz, Q. Cui, A.G. Baboul, S. Clifford, J. Cioslowski, B.B. Stefanov, G. Liu, A. Liashenko, P. Piskorz, I. Komaromi, R.L. Martin, D.J. Fox, T. Keith, M.A. Al- Laham, C.Y. Peng, A. Nanayakkara, M. Challacombe, P.M.W. Gill, B. Johnson, W. Chen, M.W. Wong, C. Gonzalez, J.A. Pople, Gaussian 03, Revision C.02, Gaussian Inc., Pittsburgh, PA, 2003.
35. K.F. Khaled, *Electrochim. Acta* 48 (2003) 2493.
36. J. Aljourani, K. Raeissi, M.A. Golozar, *Corros. Sci*. 51 (2009) 1836.
37. A.A. Aksut, W.J. Lorenz, F. Mansfeld, *Corros. Sci*. 22 (1982) 611.
38. Z.H. Tao, S.T. Zhang, W.H. Li, B.R. Hou, Corros. *Sci*. 51 (2009) 2588.
39. E.S. Ferreira, C. Giacomelli, F.C. Giacomelli, A. Spinelli, *Mater. Chem. Phys*. 83 (2004) 129.
40. S. Martinez, I. Stern, *Appl. Surf. Sci*. 199 (2008) 83.
41. P. Li, J.Y. Lin, K.L. Tan, J.Y. Lee, *Electrochim. Acta* 42 (1997) 605.
42. M. Lebrini, F. Robert, C. Roos, *Int. J. Electrochem. Sci*. 5 (2010) 1698.
43. G. Moretti, G. Quartaronr, A. Tassan, A. Zingales, *Electrochim. Acta* 41 (1996) 1971.
44. N.M. Guan, L. Xueming, L. Fei, *Mater. Chem. Phys*. 86 (2004) 59.
45. M.S. Abdel-Aal, M.S. Morad, *Br. Corros. J*. 36 (2001) 253.
46. O.K. Abialo, N.C. Oforka, *Mater. Chem. Phys*. 83 (2004) 315.
47. S.M.A. Hosseini, M. Salari, M. Ghasemi, M. Abaszadeh, *Z. Phys. Chem*. 223 (2009) 769.
48. S.A. Ali, M.T. Saeed, S.U. Rahman, *Corros. Sci*. 45 (2003) 253.
49. M.A. Migahed, *Mater. Chem. Phys*. 93 (2005) 48.
50. I. Ahamad, R. Prasad, M.A. Quraishi, *Corros. Sci*. 52 (2010) 933.
51. E.A. Noor, A.H. Al-Moubaraki, *Mater. Chem. Phys*. 110 (2008) 145.
52. M. Özcan, R. Solmaz, G. Kardas, I. Dehri, *Colloids Surf. A* 325 (2008) 57.

53. R. Solmaz, *Corros. Sci*. 52 (2010) 3321.
54. A. Döner, R. Solmaz, M. Özcan, G. Kardas, *Corros. Sci*. 53 (2011) 2902.
55. G. Moretti, F. Guidi, G. Grion, *Corros. Sci*. 46 (2004) 387.
56. M. Bouklah, N. Benchat, B. Hammouti, A. Aouniti, S. Kertit, *Mater. Lett*. 60 (2006) 1901.
57. N. Khalil, *Electrochim. Acta* 48 (2003) 2635.
58. J. Zhang, J. Liu, W. Yu, Y. Yan, L. You, L. Liu, *Corros. Sci*. 52 (2010) 2059.
59. M. Lebrini, M. Lagrenee, M. Traisnel, L. Gengembre, H. Vezin, F. Bentiss, *Appl. Surf. Sci*. 253 (2007) 9267.
60. V.S. Sastri, J.R. Perumareddi, *Corrosion*, 53 (1997) 671.
61. R.G. Pearson, *Inorg. Chem*. 27 (1988) 734.
62. S. Martinez, *Mater. Chem. Phys*. 77 (2002) 97.
63. I. Lukovits, E. Kalman, F. Zucchi, *Corrosion*, 57 (2001) 3.